Supplementary Information (SI) for Reaction Chemistry & Engineering.
This journal is © The Royal Society of Chemistry 2024

Electronic Supplementary Information

Boosting the electrocatalytic activity of $LaCoO_3$ core–shell hollow sphere for oxygen evolution reaction through modulating inner oxygen vacancies

Long Li, Jinbo Guo, Jiang Shen and Qiang Hu*

Department of Chemistry, Lishui University, Lishui 323000, P. R. China.

E-mail: qihu@z-etech.cn

1 Materials characterizations

The phase formation was identified using powder X-ray diffraction (XRD) (Bruker D8, Cu-Kα). The morphologies of the catalysts were observed by field emission scanning electron microscopy (FE-SEM, HITACHI S-4800) and transmission electron microscopy (TEM, JEOL JEM-2010). The linear scanning energy-dispersive X-ray spectrometry (EDX) and EDX elemental mappings were taken on TEM. The X-ray photoelectron spectroscopy (XPS) spectra were measured on ESCALAB 250 spectrometer (Perkin-Elmer). Electron paramagnetic resonance (EPR) spectra were performed using a Bruker ESR spectrometer (JES-FA200).

2 Electrochemical measurements

The electrochemical tests were conducted on CHI 760E electrochemical workstation. The Ag/AgCl (saturated KCl solution) as used as the reference electrode, a graphite rod was served as the counter electrode, and all NiO spheres catalysts were utilized as working electrode. All electrochemical tests were performed in 1 M KOH aqueous electrolyte and the catalysts were dissolved in ethanol solution and then uniformly cast onto glassy carbon working electrode with a total loading of 0.4 mg cm^{-2}. All the linear sweep voltammetry (LSV) measurements were taken at a scan rate of 5 mV s^{-1} to obtain the polarization curves. Chronoamperometric measurements were performed at corresponding potential to deliver a current density of 10 mA cm^{-2}. The Tafel slope was calculated according to the Tafel equation $\eta = b \log (j/j_0)$ (η is the overpotential, b is the Tafel slope, j is the current density, and j_0 is the exchange current density). Potentials were referenced to a reversible hydrogen electrode (RHE) using the following equation: Potentials were referenced to a reversible hydrogen electrode (RHE) using the following equation: E (RHE) =E (Ag/AgCl) + (0.205 + 0.059pH) V. The electrochemical impedance spectroscopy (EIS) measurements were carried out by ranging the frequency from 100 k Hz to 0.1 Hz.

2. Supplementary figures

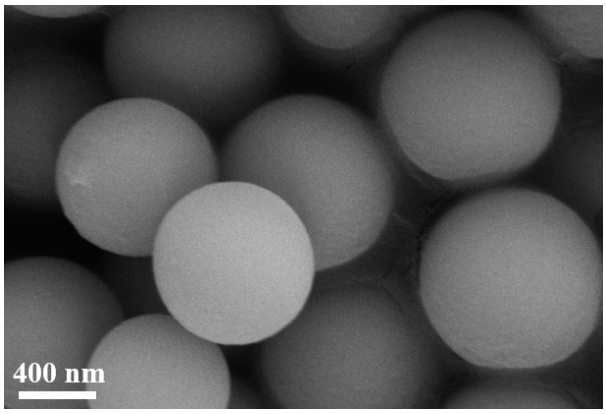

Fig. S1 SEM image of the LaCo-precursor sample.

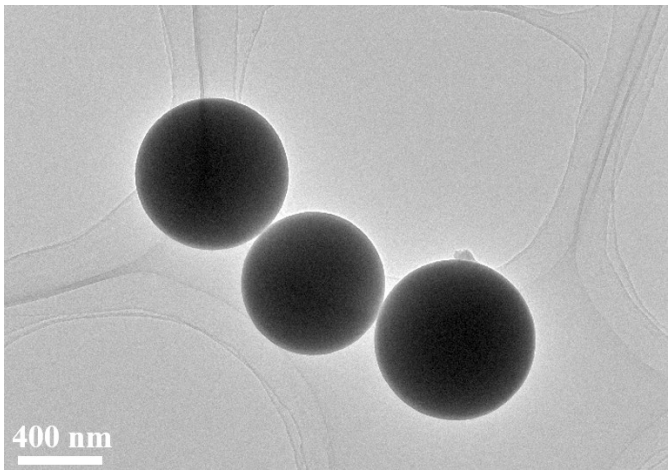

Fig. S2 TEM image of the LaCo-precursor sample.

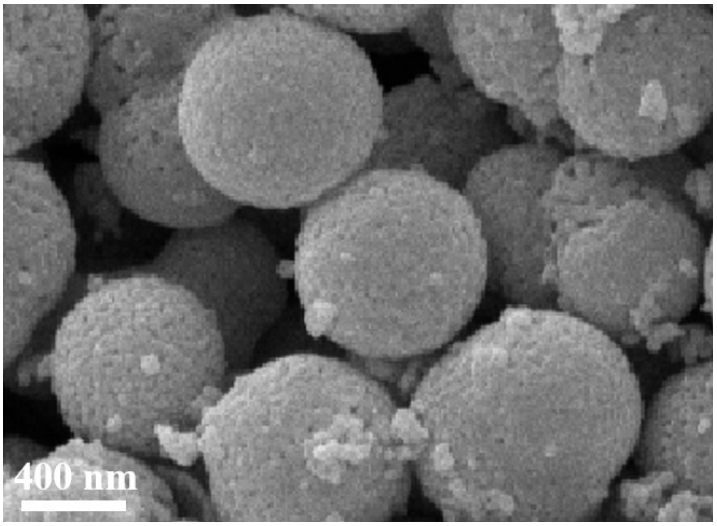

Fig. S3 SEM image of the $LaCoO_3$ core-shell hollow spheres.

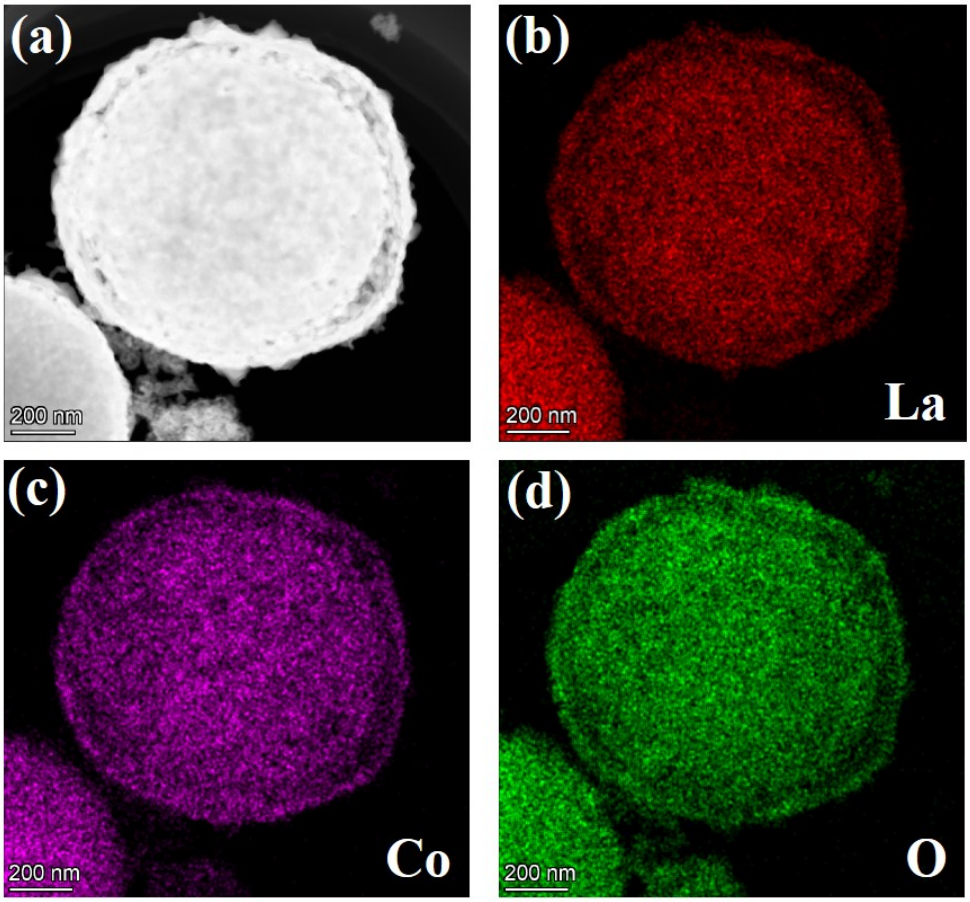

Fig. S4 (a) High resolution TEM image, (b) La mapping, (c) Co mapping and (d) O mapping of an individual $LaCoO_{3-x}$-M core-shell sphere.

One $LaCoO_{3-x}$-M core-shell sphere has been randomly picked and the core-shell morphology was examined by high resolution TEM (HR-TEM, Fig. S4a). The elemental mapping is carried out, and the La, Co, and O elements are clearly identified as shown in Fig. S4b-d.

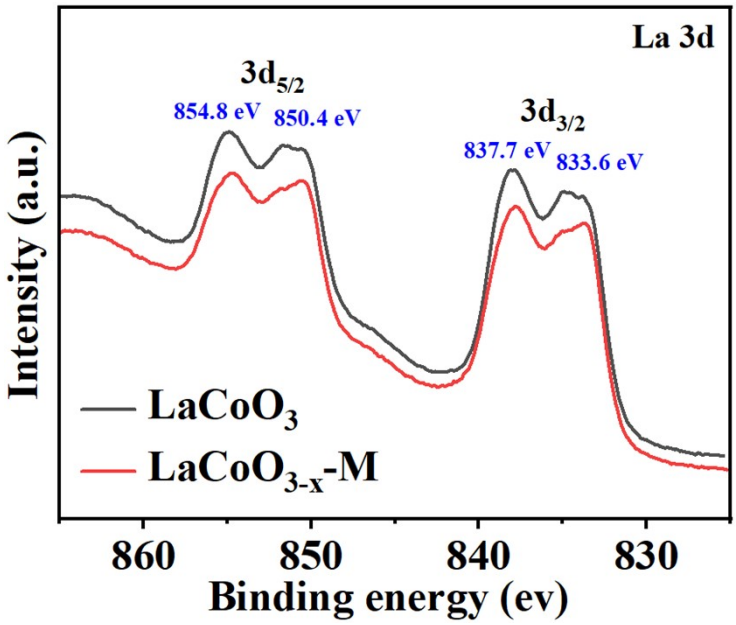

Fig. S5 High-resolution XPS spectrum of La 3d for $LaCoO_3$ and $LaCoO_{3-x}$-M spheres.

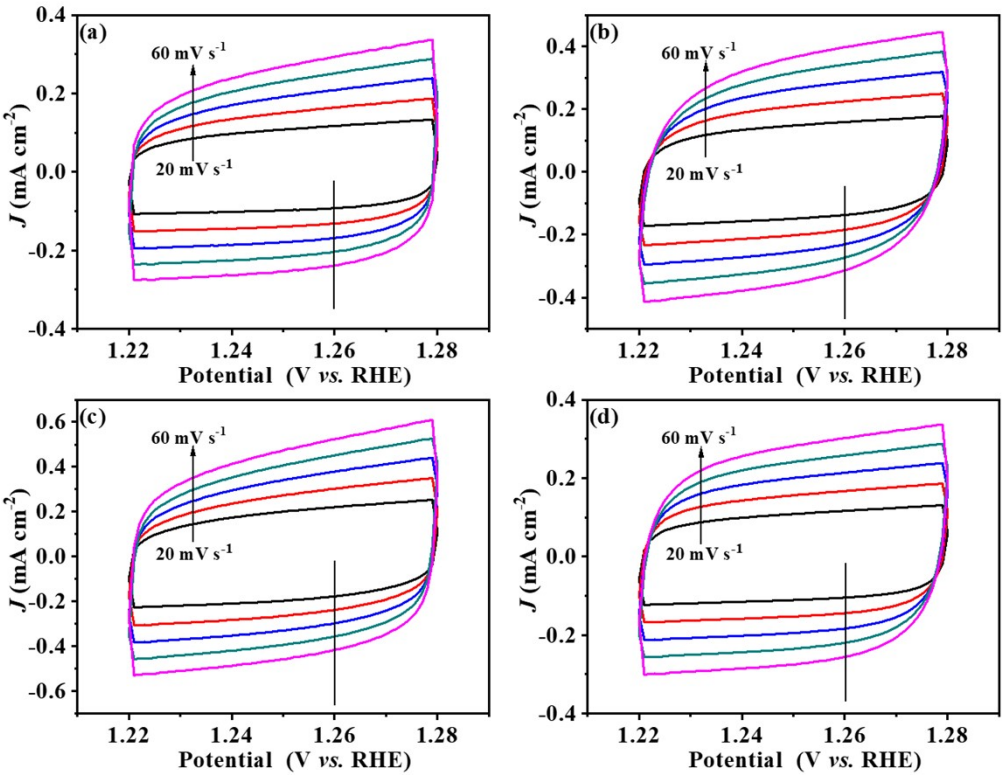

Fig. S6 CVs tested at the potential range of 1.22 –1.28 V vs. RHE with the scan rates increasing from 20 to 60 mV s^{-1} for (a) $LaCoO_3$, (b) $LaCoO_{3-x}$-L, (c) $LaCoO_{3-x}$-M and (d) $LaCoO_{3-x}$-H spheres.

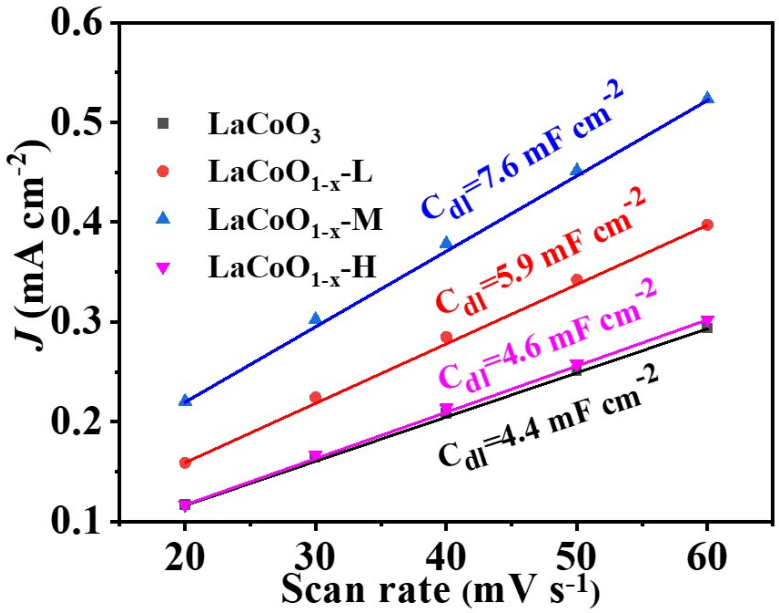

Fig. S7 Plots of the current density at 1.26 V (vs. RHE) vs. the scan rate of $LaCoO_3$, $LaCoO_{3-x}$-L, $LaCoO_{3-x}$-M and $LaCoO_{3-x}$-H spheres.

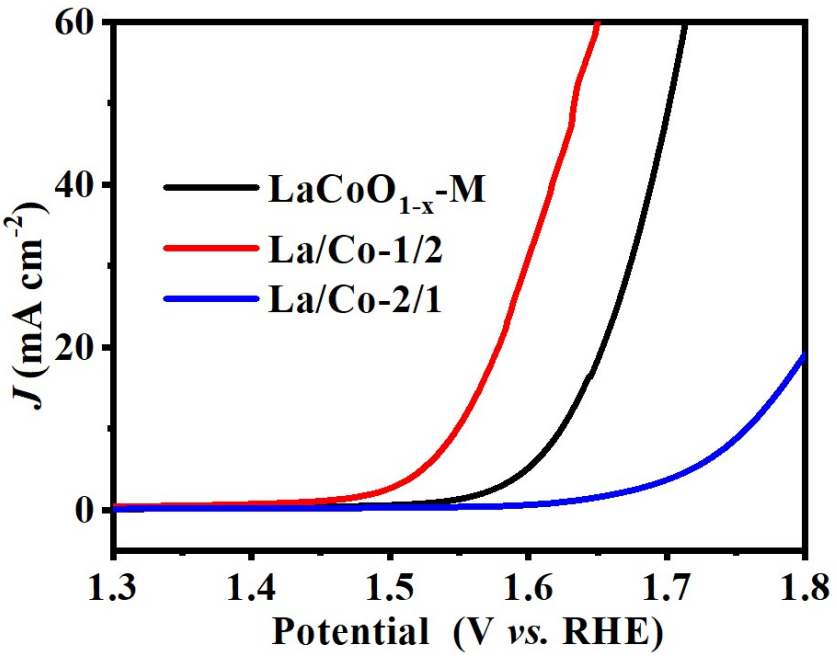

Fig. S8 Polarization curves of $LaCoO_{3-x}$-M, La/Co-1/2 and La/Co-2/1 spheres in an O_2-saturated 1.0 M KOH solution (scan rate of 2 mV s^{-1}).

The electrocatalytic performance with different La and Co in the $LaCoO_{3-x}$ core–shell spheres was further evaluated via the linear sweep voltammetry. As shown in Fig. S8, when the ratio of La to Co is 1 to 2, the La/Co-1/2 spheres exhibited a higher catalytic activity than the $LaCoO_{3-x}$-M spheres. In addition to $LaCoO_3$, cobalt oxide may be produced as a product when the ratio of La to Co is 1 to 2. And the higher catalytic activity may originate from cobalt oxide, which usually has better catalytic performance compared to $LaCoO_3$. Further when the ratio of La to Co is 2 to 1, the La/Co-2/1 spheres exhibited a lower catalytic activity than the $LaCoO_{3-x}$-M spheres. In addition to $LaCoO_3$, lanthanum oxide may be produced as a product when the ratio of La to Co is 2 to 1. The presence of lanthanum oxide may lead to a decrease in catalytic activity. Considering that more cobalt in the $LaCoO_{3-x}$ core–shell spheres leads to better catalytic activity, cobalt should be the active center. This can be confirmed by the XPS spectrum of the $LaCoO_{3-x}$-M spheres before and after electrolysis. As shown in Fig. S9a, the ratio of Co^{3+} in $LaCoO_{3-x}$-M spheres increased after electrolysis, demonstrating that higher valence cobalt species are produced after catalysis (such as CoOOH).[1, 2] And the appearance of the O4 peak (M-OH) in XPS spectrum of O 1s (Fig. S9b) for the $LaCoO_{3-x}$-M spheres after catalysis further proves the production of CoOOH after catalysis.[3, 4] Furthermore, the almost unchanged La 3d XPS spectrum of the $LaCoO_{3-x}$-M spheres before and after electrolysis (Fig. S9c) further proves that cobalt should be the active center rather than lanthanum.

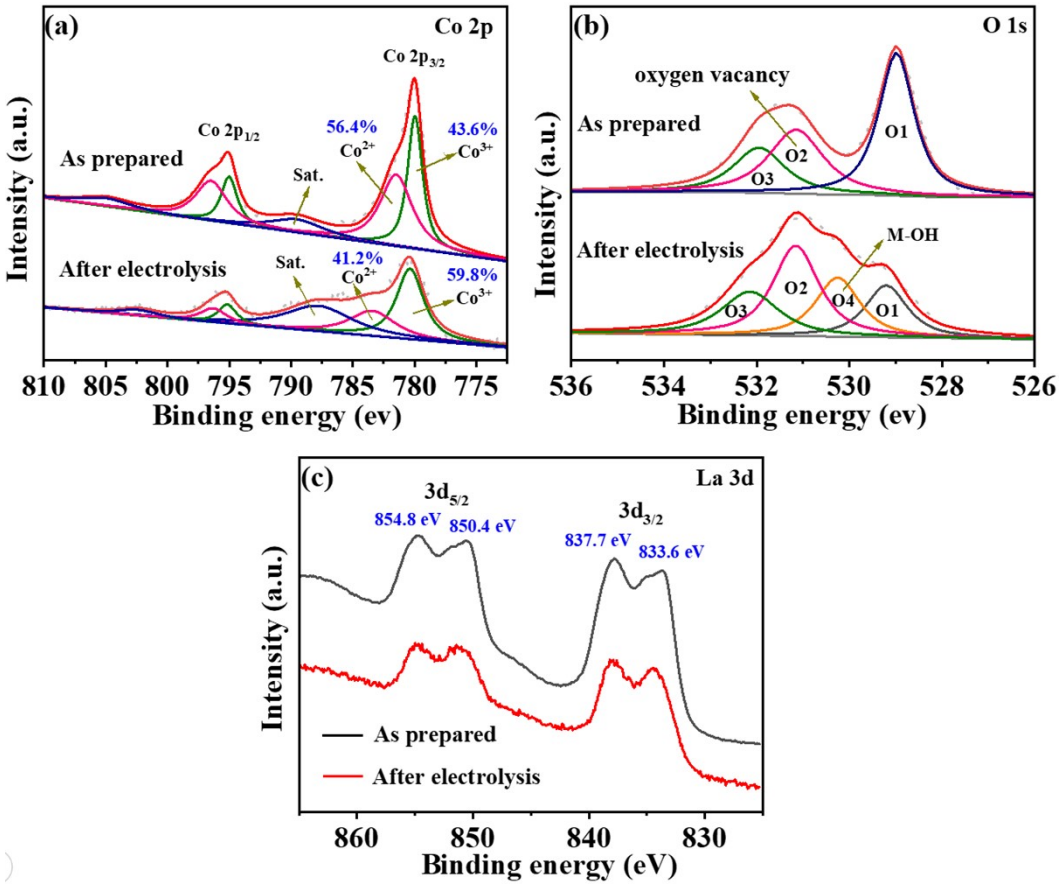

Fig. S9 High-resolution XPS spectrum of (a) Co 2p, (b) O 1s, (c) La 3d for the $LaCoO_{3-x}$-M spheres before and after electrolysis.

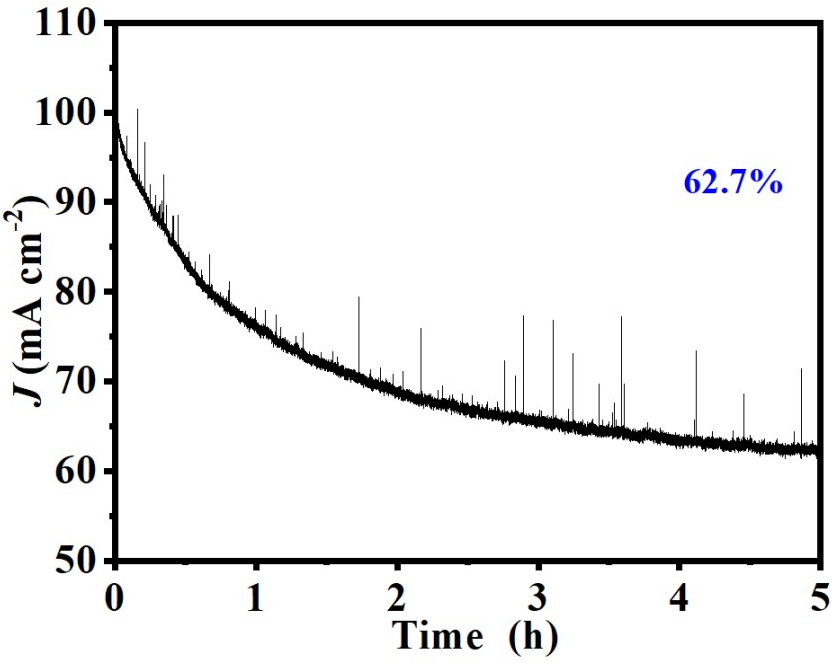

Fig. S10 Chronoamperometric response at a current density of 100 mA cm^{-2} for 5 hours for $LaCoO_{3-x}$-M spheres.

The stability test at higher current density of 100 mA cm^{-2} was performed. As shown in Fig.S10, $LaCoO_{3-x}$-M spheres demonstrated huge drop in current density after 5 hours of continuous operation, and the unsatisfactory performance may come from the fact that the larger current density leads to the production of a large number of bubbles, resulting in severe catalyst shedding.

1. K. Zhu, X. Zhu and W. Yang, *Angew. Chem. Int. Ed.*, 2019, **58**, 1252-1265.
2. X. Zhang, S. Liu, Y. Zang, R. Liu, G. Liu, G. Wang, Y. Zhang, H. Zhang and H. Zhao, *Nano Energy*, 2016, **30**, 93-102.
3. L. Liardet and X. Hu, *ACS Cataly.*, 2019, **9**, 5522-5522.
4. H. Ali-Löytty, M. W. Louie, M. R. Singh, L. Li, H. G. Sanchez Casalongue, H. Ogasawara, E. J. Crumlin, Z. Liu, A. T. Bell, A. Nilsson and D. Friebel, *The Journal of Physical Chemistry C*, 2016, **120**, 2247-2253.